Performance Analysis of Single Step Co-Fired Solid Oxide Fuel Cells (SOFCs)

Kyung Joong Yoon, Peter A. Zink, Uday B. Pal, Srikanth Gopalan

Department of Mechanical Engineering
Division of Materials Science and Engineering
Boston University

OUTLINE

- Introduction
- Single Step Co-firing Process Development
- Polarization Modeling
- Polarization Analysis
- Fuel Utilization Test
- Advanced Cathode Investigation
- Summary & Future Work

INTRODUCTION

❖ **Major Challenges for Commercialization of SOFCs**

High Manufacturing Costs (SOFC System Costs per Unit of Power ($/kW))	**Reduced Cell Performance at Low Operating Temperature** (Interconnects, Sealing, etc.)
⇩	⇩
Single Step Co-Firing Process with Conventional Material System	**Polarization Modeling**: Systematic Analysis of Cell Performance and Polarization Losses

❖ **Research Goals**

- Manufacture SOFCs with the Lowest Manufacturing Costs

  by **Single Step Co-Firing of the Entire SOFCs**

- Achieve the Highest Cell Performance and Lower Operating Temperature

  by **Optimization of Materials, Microstructures, and Process Parameters using Polarization Modeling**

⇒ **Minimize $/kW**

SINGLE STEP CO-FIRING PROCESS

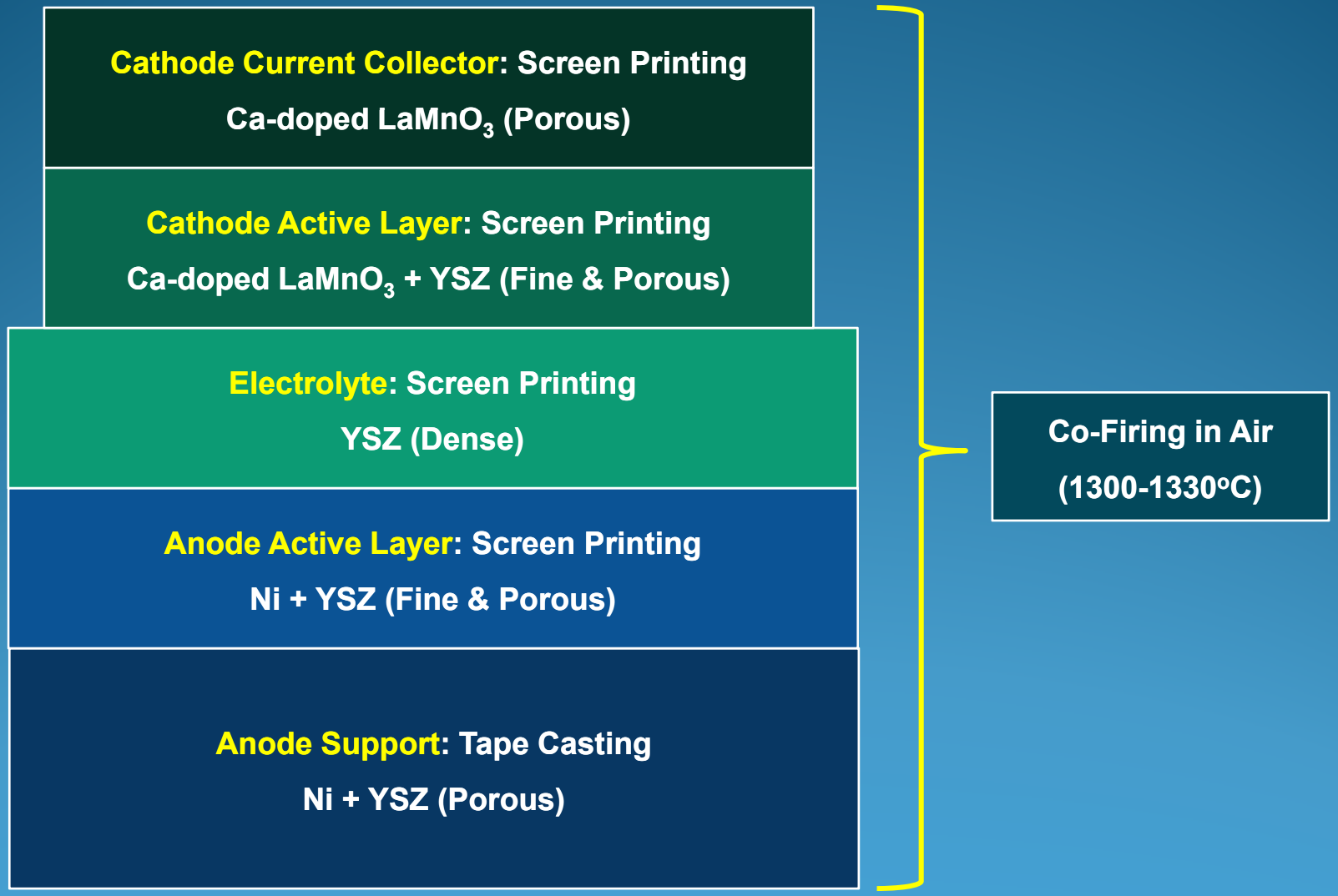

PROCESS DEVELOPMENT

- Lowered Electrolyte Sintering Temperature
  - Density of YSZ : Without Sintering Aid: ~ 94%, With Sintering Aid: ~ 99+% @1300°C
- Matched Thermal Expansion Coefficients and Sintering Shrinkages
- Developed Refractory Cathode Composition
  - Doped-$(La,Ca)MnO_3$

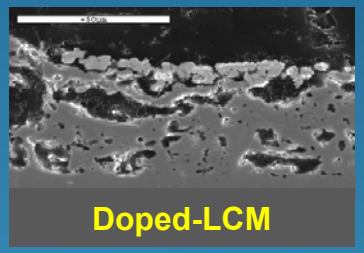
Doped-LCM

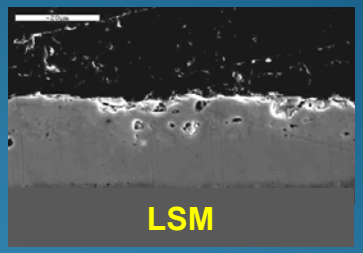
LSM

- Optimized Thicknesses and Porosities of Electrodes
- Optimized Particle Sizes of Initial Powders
- Evaluated Pore Former Material
  - Carbon Black

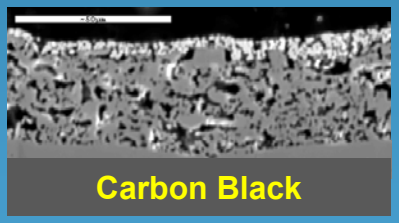
Carbon Black

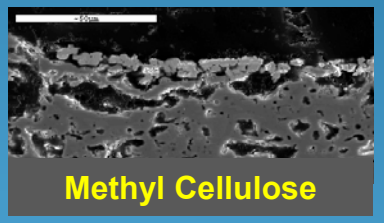
Methyl Cellulose

- Employed Cathode Current Collector

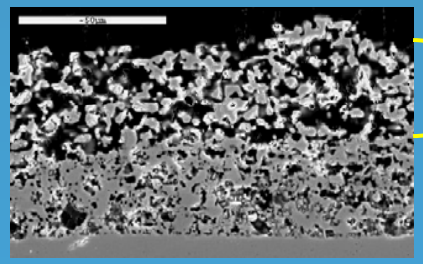

Cathode Current Collector
: $(La,Ca)MnO_3$
50μm thick, 50% porous

PROCESS DEVELOPMENT

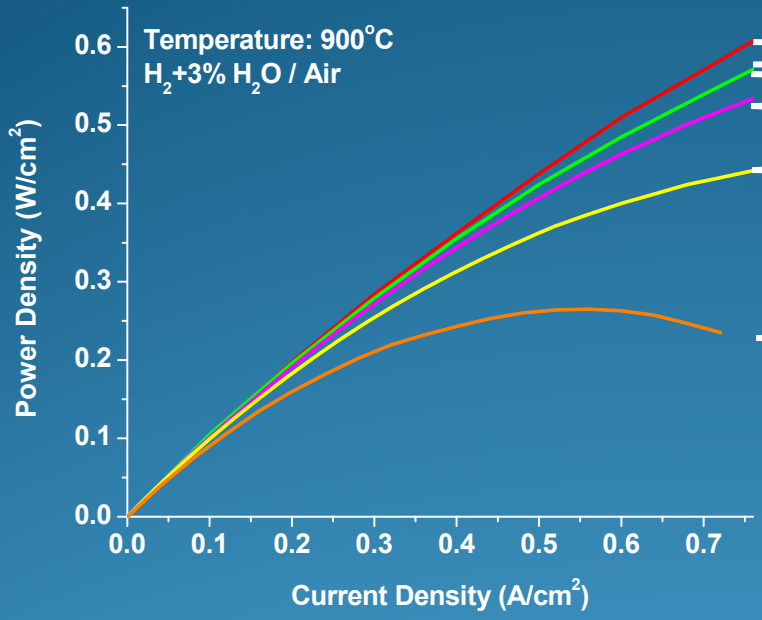

- Cathode Particle Size Optimization
- Cathode Current Collector
- Anode Porosity Optimization
- Pore Former Material Optimization

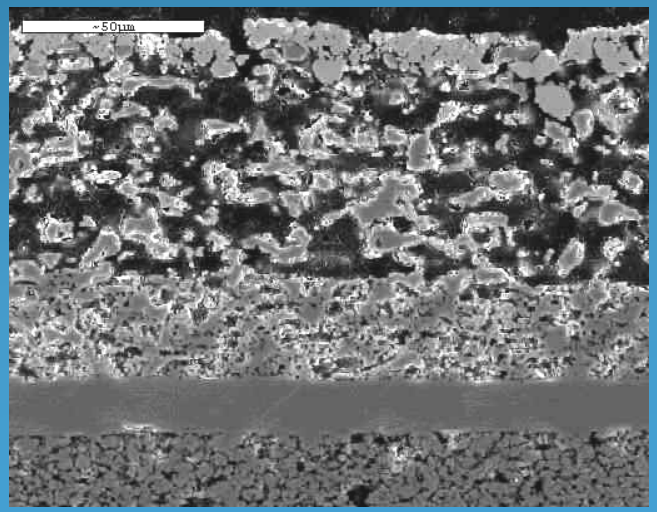

Cathode Current Collector:
LCM, 50μm thick, 50% porous

Cathode Active Layer:
LCM-YSZ, 30μm thick, 31% porous

Electrolyte: YSZ, 15μm thick

Anode Support:
Ni-YSZ, 850μm thick, 32% porous

BASELINE CELL: POWER DENSITY

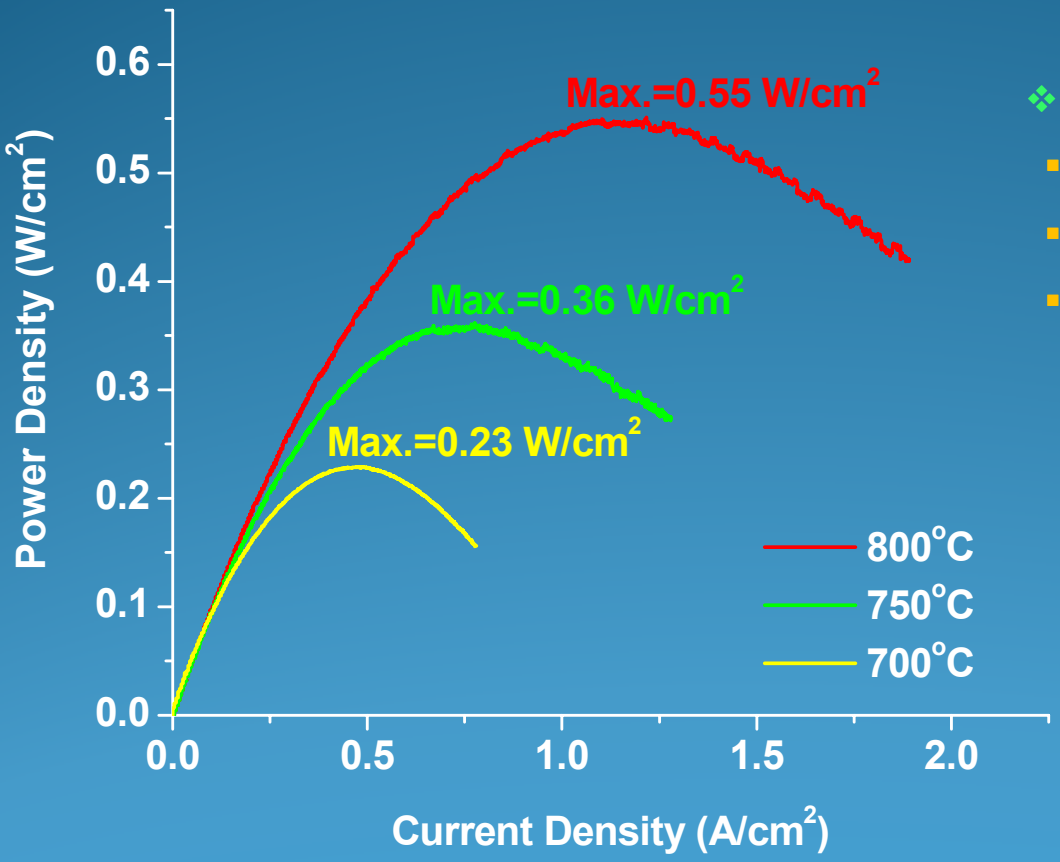

- **Test Condition**
  - Temperature: 700~800°C
  - Fuel: 97% H_2+3% H_2O
  - Oxidant: Air

POLARIZATION MODEL: THEORY

$$E_C = E_0 - iR_i - \eta_{act} - \eta_{conc}$$

- **Activation Polarization (η_{act})*** : $i = i_0 \exp\left(\frac{\alpha n_e \eta_{act} F}{RT}\right) - i_0 \exp\left(-\frac{(1-\alpha) n_e \eta_{act} F}{RT}\right)$ (α=1/2, n_e=2)

$$\eta_{act} = \frac{RT}{F} \ln\left\{\frac{1}{2}\left[\left(\frac{i}{i_0}\right) + \sqrt{\left(\frac{i}{i_0}\right)^2 + 4}\right]\right\} \quad \text{(Anode + Cathode)}$$

- **Concentration Polarization (η_{conc})**** : $\eta_{conc} = -\frac{RT}{4F}\ln\left(1-\frac{i}{i_{cs}}\right) - \frac{RT}{2F}\ln\left(1-\frac{i}{i_{as}}\right) + \frac{RT}{2F}\ln\left(1+\frac{p^o_{H_2} i}{p^o_{H_2O} i_{as}}\right)$

$$E_C = E_o - iR_i - \frac{RT}{F}\ln\left\{\frac{1}{2}\left[\left(\frac{i}{i_o}\right) + \sqrt{\left(\frac{i}{i_o}\right)^2 + 4}\right]\right\} + \frac{RT}{4F}\ln\left(1-\frac{i}{i_{cs}}\right) + \frac{RT}{2F}\ln\left(1-\frac{i}{i_{as}}\right) - \frac{RT}{2F}\ln\left(1+\frac{p^o_{H2} i}{p^o_{H2O} i_{as}}\right)$$

Open Circuit Potential	Ohmic Polarization	Activation Polarization	Concentration Polarization (Cathode)	Concentration Polarization (Anode)

* P.W.Li, M.K.Chyu, *J. Heat Transfer*, vol.127, 1344 (2005)

** J.W.Kim, A.V.Virkar, K-Z.Fung, K.Mehta, S.C.Singhal, *J.Electrochem.Soc.*146 (1) (1999) 69

POLARIZATION MODELING: CURVE-FITTING (EXAMPLE)

❖ **Test Condition**

- Temperature: 800°C
- Fuel: 97% H_2+3% H_2O (300cc/min): Fixed
- Oxidant: 100%, 21%, 8% O_2 + N_2 (1000cc/min)

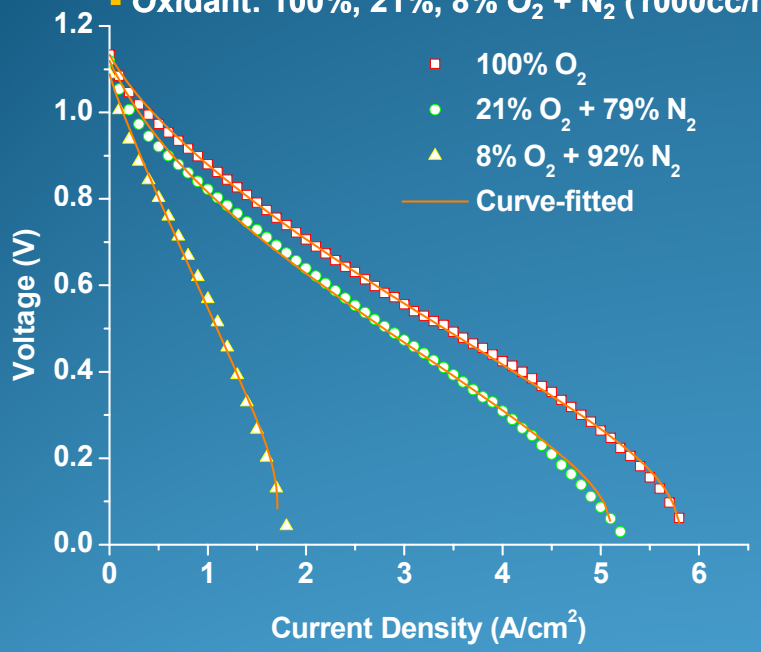

Fitting Parameters	100% O_2	21% O_2 + 79% N_2	8% O_2 + 92% N_2
R_i (Ω·cm²)	0.082	0.082	0.082
i_o (A/cm²)	0.52	0.28	0.097
i_{as} (A/cm²)	5.77	5.77	5.77
i_{cs} (A/cm²)	-	5.42	1.77

Assumption: $i_{cs} >> i_{as}$ and $\eta_{conc,c} << \eta_{conc,a}, \eta_{act}$ with 100% O_2

- Anode Limiting Current $$i_{as} = \frac{2 F p^{o}_{H2} D^{eff}_{H2-H2O}}{R T l_a}$$

$D^{eff}_{H2\text{-}H2O} = 0.23$ cm²/s

- Cathode Limiting Current $$i_{cs} = \frac{4 F p^{o}_{O2} D^{eff}_{O2-N2}}{\left(\frac{p - p^{o}_{O2}}{p}\right) R T l_c}$$

$D^{eff}_{O2\text{-}N2} = 0.037$ cm²/s

POLARIZATION MODELING: VERIFICATION OF ASSUMPTION

Various Polarization Losses @800°C with Humidified Hydrogen (3% H_2O) and Air

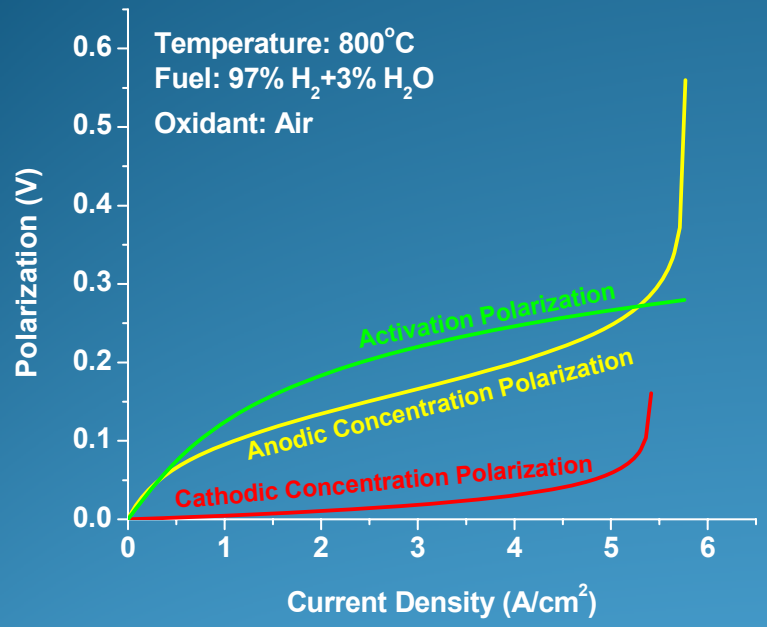

Cathodic Limiting Current Density @800°C as a Function of p_{O2} in Oxidant

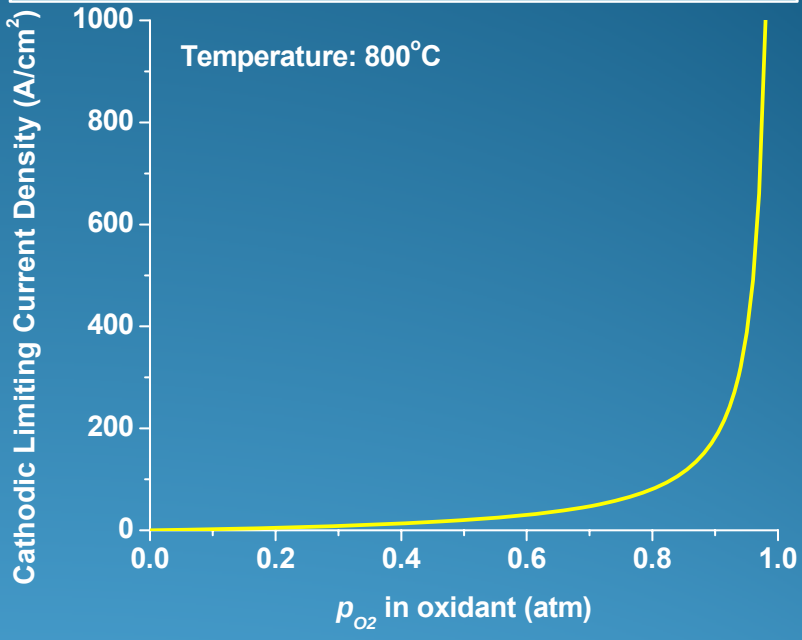

- $\eta_{conc,c}$ << $\eta_{conc,a}$ and η_{act} except at high current density near i_{cs}

- i_{cs} rapidly increases as p_{O2} increases and approaches 100% O_2

❖ **Consistent with assumption that $\eta_{conc,c}$ is negligible compared to other polarization losses when oxygen at the cathode nears 100%**

Polarization Modeling & Impedance Spectroscopy

- **Activation Polarization Resistance at OCV**

$$R_{act} = \frac{d\eta_{act}}{di} = \frac{RT}{F} \cdot \frac{1}{\sqrt{i^2 + 4i_o^2}}$$

$$R_{act}|_{i \to 0} = \frac{RT}{2Fi_o}$$

- **Anodic Concentration Polarization Resistance at OCV**

$$R_{conc,a} = \frac{d\eta_{conc,a}}{di} = \frac{RT}{2F}\left[\frac{1}{i_{as}\left(1 - \frac{i}{i_{as}}\right)} + \frac{p^o_{H2}}{p^o_{H2O}} \cdot \frac{1}{i_{as}\left(1 + \frac{p^o_{H2}}{p^o_{H2O}} \cdot \frac{i}{i_{as}}\right)}\right]$$

$$R_{conc,a}|_{i \to 0} = \frac{RT}{2F} \cdot \frac{1}{i_{as}}\left(1 + \frac{p^o_{H2}}{p^o_{H2O}}\right)$$

- **Cathodic Concentration Polarization Resistance at OCV**

$$R_{conc,c} = \frac{d\eta_{conc,c}}{di} = \frac{RT}{4F} \cdot \frac{1}{i_{cs}\left(1 - \frac{i}{i_{cs}}\right)}$$

$$R_{conc,c}|_{i \to 0} = \frac{RT}{4F} \cdot \frac{1}{i_{cs}}$$

Impedance Spectroscopy @800°C

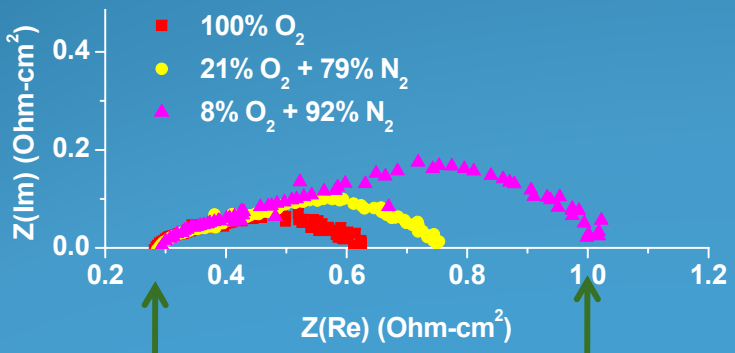

High Frequency Intercept = R_Ω

Low Frequency Intercept = $R_{polar} + R_\Omega$

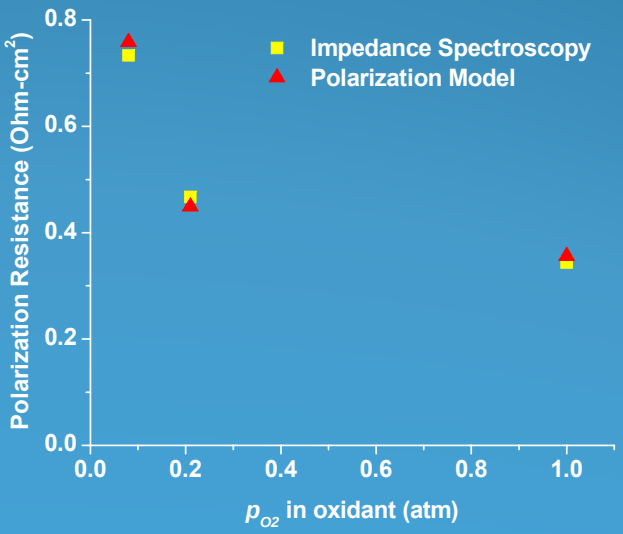

POLARIZATION ANALYSIS #1: BASELINE CELL

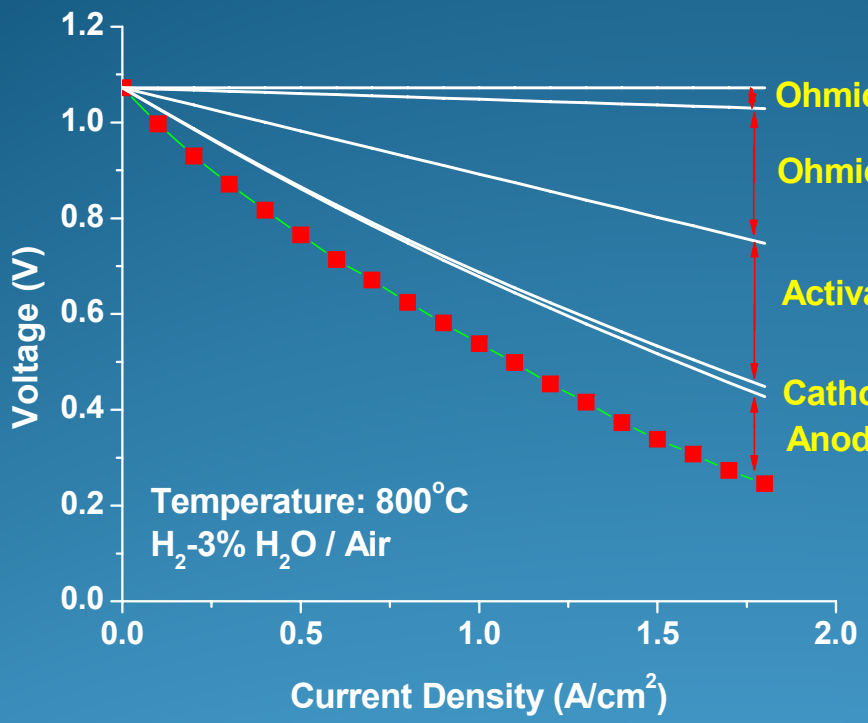

Ohmic Loss (Electrolyte)

Ohmic Loss (Electrode) : Anode + Cathode + Contacts

Activation Polarization

Cathodic Concentration Polarization

Anodic Concentration Polarization

- Dominant Polarization Losses
  - Ohmic Loss (Electrode)
  - Activation Polarization (Cathode)
  - Concentration Polarization (Anode)

POLARIZATION ANALYSIS #2: CONTACT RESISTANCE

❖ Cathode Current Collection : Ag Mesh vs. Pt Mesh

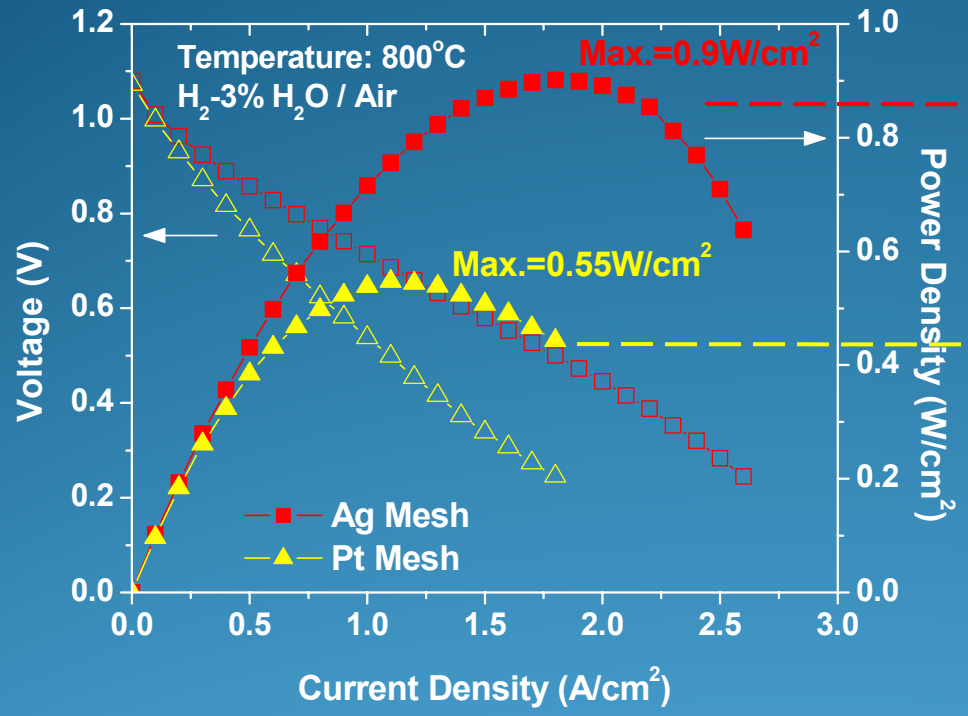

T_m(Ag) = 961°C

$R_{electrode}$ = 0.067 Ω·cm²

T_m(Pt) = 1772°C

$R_{electrode}$ = 0.156 Ω·cm²

- Ag is softer than Pt at operating temperature.

  ⇒ Higher Interfacial Contact Area ⇒ Lower Ohmic Electrode Resistance

- In SOFC stacks, the effect of the contacts between the electrode and interconnects can be substantial.

Polarization Analysis #3: Cathode Microstructure

❖ **Sintering Temperature: 1300°C vs. 1330°C**

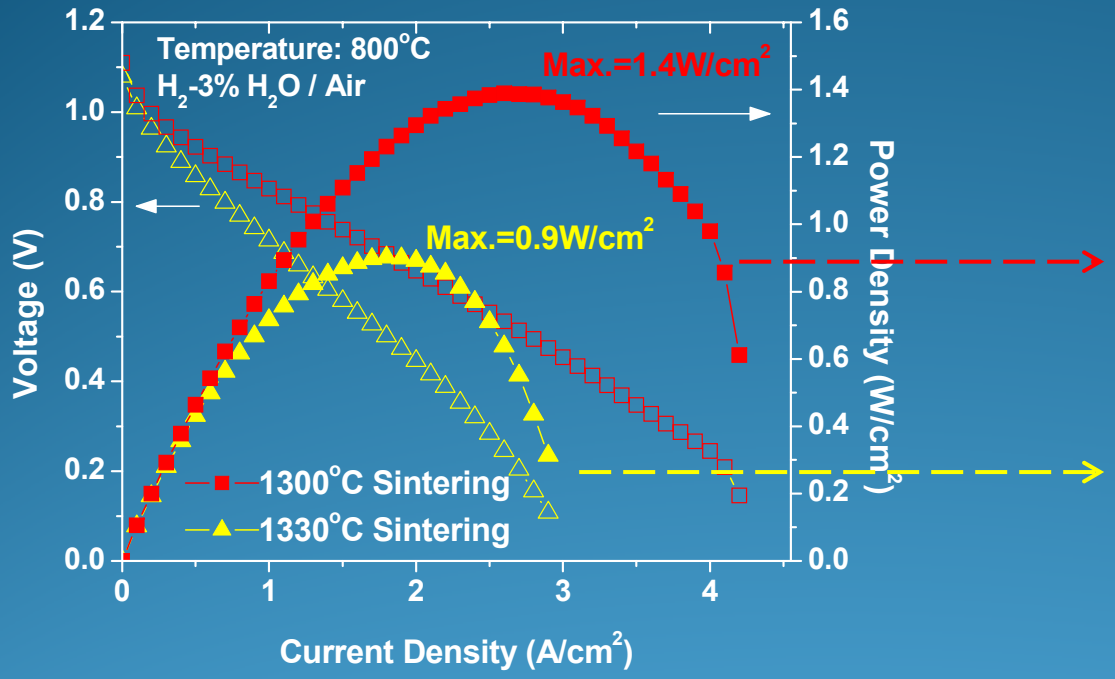

1300°C Sintering

Avg. Grain Size = 2.3 μm

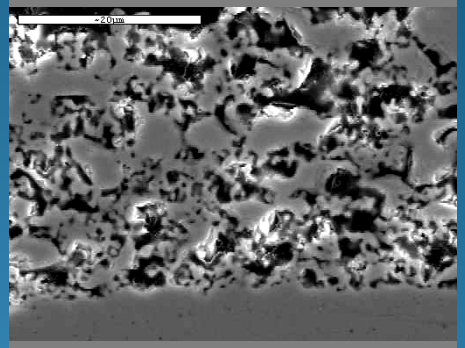

i_o = 0.27 A/cm²

1330°C Sintering

Avg. Grain Size = 3.2 μm

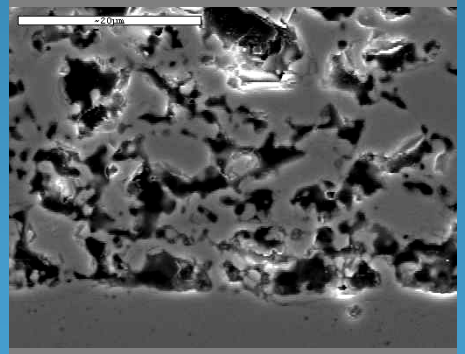

i_o = 0.16 A/cm²

Impedance Spectroscopy

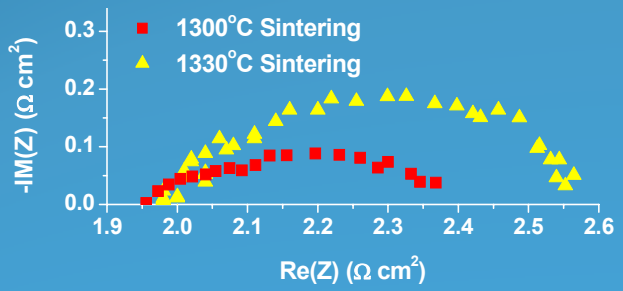

- No Significant Change in Anode Microstructure.
- Less Sintering of Cathode ⇒ Low Activation Polarization

POLARIZATION ANALYSIS #4: ANODE POROSITY

- Pore Former in Anode: 8 wt% C vs. 5 wt% C

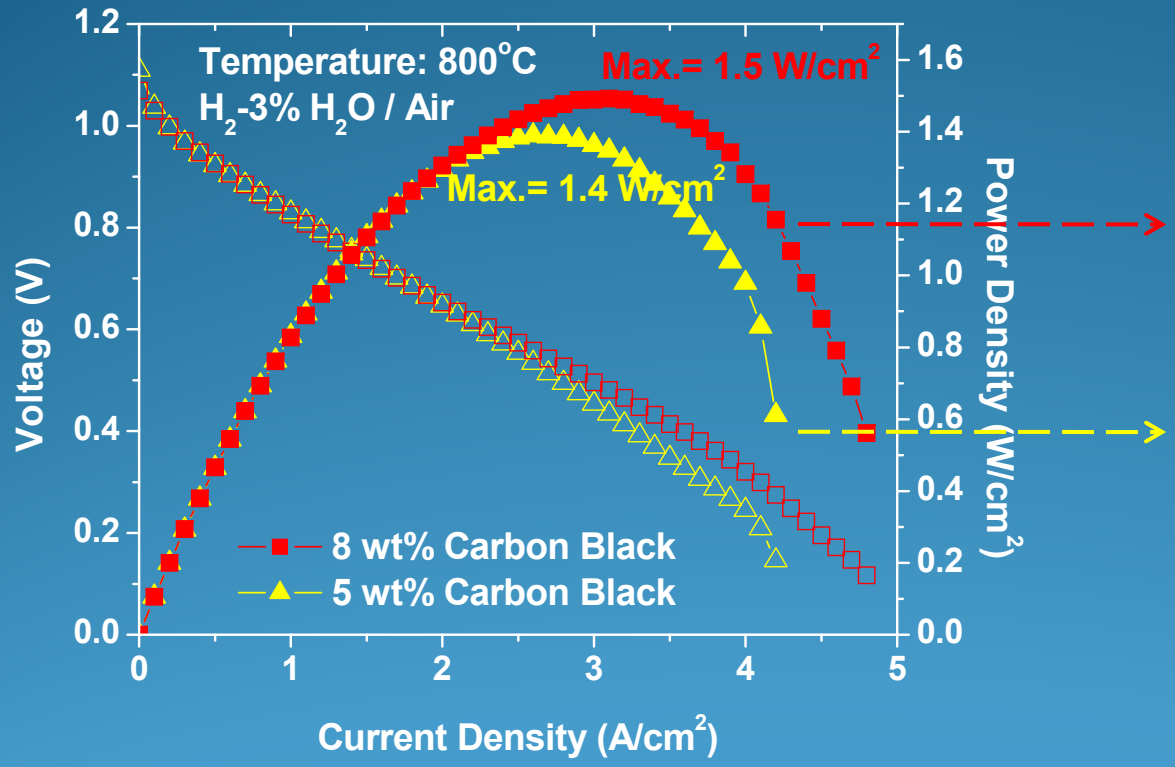

8 wt% Carbon Black

Anode Porosity: 37%

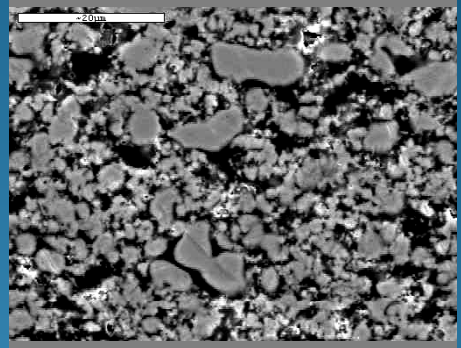

i_{as} = 5.77 A/cm²

$D^{eff}_{H2\text{-}H2O}$ = 0.23 cm²s⁻¹

5 wt% Carbon Black

Anode Porosity: 32%

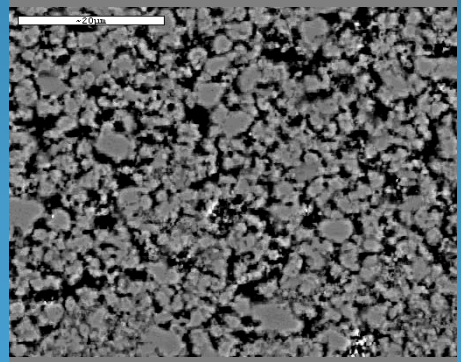

i_{as} = 4.97 A/cm²

$D^{eff}_{H2\text{-}H2O}$ = 0.19 cm²s⁻¹

- Increased Anode Porosity

  ⇒ Low Anode Concentration Polarization

Cell Performance Improvement Chart

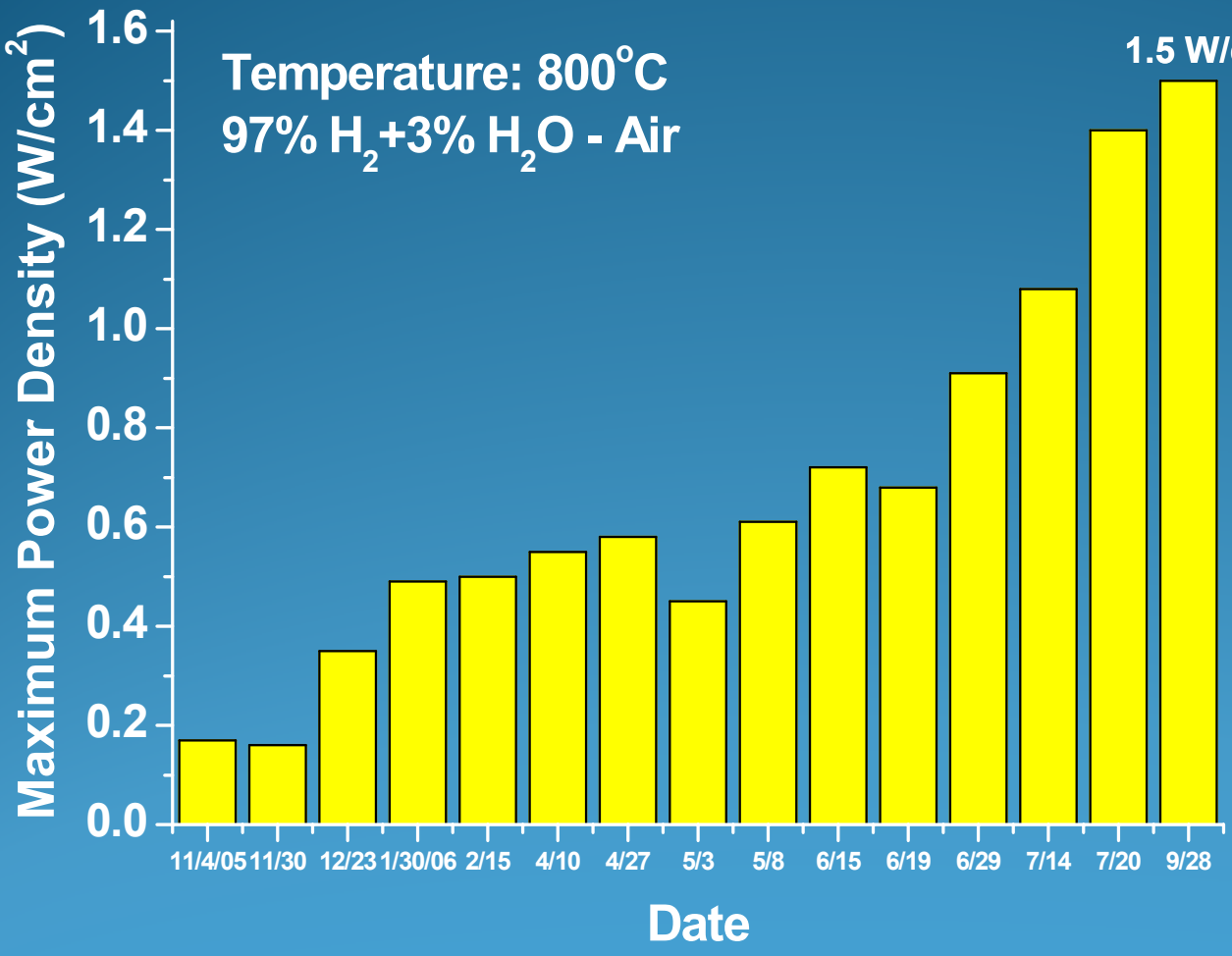

Comparable to the State-of-the-Art Cells Fabricated with Multiple Firing Steps

Fuel Utilization Test : Background

- **Fuel Utilization**

$$U_t = \frac{\text{Molar flow rate of reactants consumed in a cell}}{\text{Molar flow rate of reactants supplied into the cell}} = \frac{\dot{N}_{consumed}}{\dot{N}_{in}}$$

- **Fuel utilization increases along the flow path over the electrode surface.**

  ⇐ Fuels are consumed and products are formed along the flow path.

- **Cell Performance Loss near Exit (High Fuel Utilization)**
  - **Loss of Nernst Potential**
  - **Anodic Activation Polarization**
  - **Anodic Concentration Polarization**

- **Simulate the effect of practical fuel utilization on single cell performance by increasing H_2O content in fuel**

Fuel Utilization Test : Effect of Anode Active Layer

With Anode Active Layer

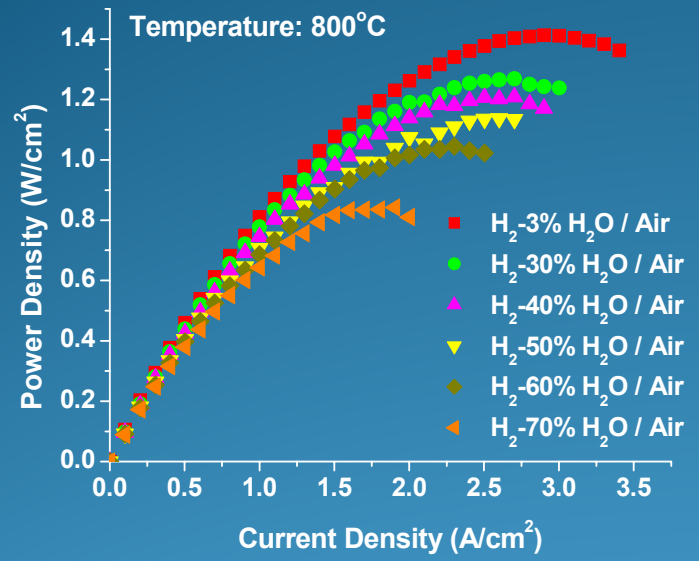

Without Anode Active Layer

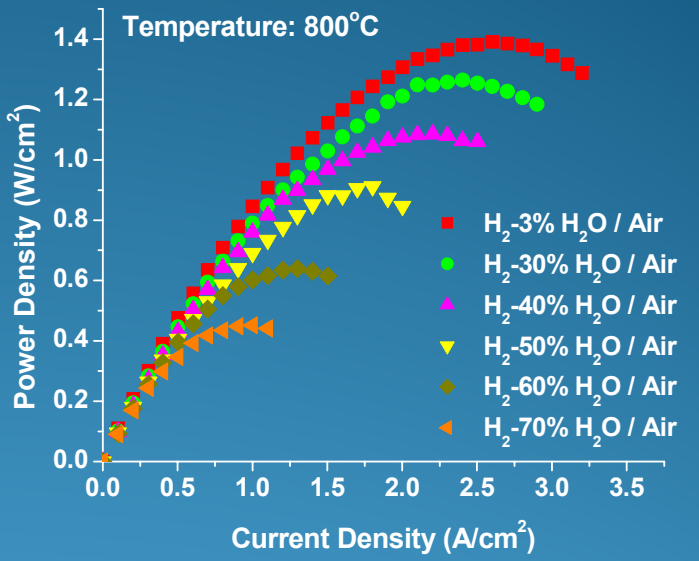

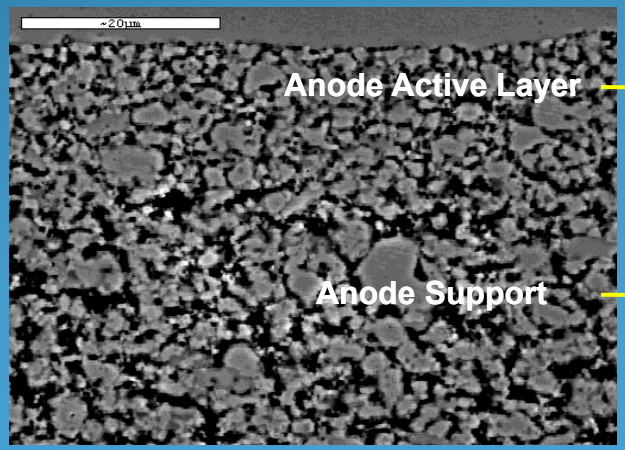

Porosity = 26%
Avg. Grain Size = 1.3 μm
Avg. Pore Size = 0.7 μm

Porosity = 37%
Avg. Grain Size = 4.3 μm
Avg. Pore Size = 2.6 μm

Fuel Compositions	Max. Power Density (W/cm²)	
	With AAL	Without AAL
H_2 – 3% H_2O	1.41	1.40
H_2 – 30% H_2O	1.27	1.25
H_2 – 50% H_2O	1.17	0.91
H_2 – 70% H_2O	0.84	0.45

Fuel Utilization Test : Polarization Modeling

$$E_C = E_o - iR_i - \frac{2RT}{F}\ln\left\{\frac{1}{2}\left[\left(\frac{i}{i_o}\right) + \sqrt{\left(\frac{i}{i_o}\right)^2 + 4}\right]\right\} + \frac{RT}{4F}\ln\left(1 - \frac{i}{i_{cs}}\right) + \frac{RT}{2F}\ln\left(1 - \frac{i}{i_{as}}\right) - \frac{RT}{2F}\ln\left(1 + \frac{p^o_{H2}i}{p^o_{H2O}i_{as}}\right)$$

R_i, $D^{eff}_{O2\text{-}N2}$: Independent of Fuel Composition

$D^{eff}_{H2\text{-}H2O}$: Independent of H_2/H_2O ratio (Kinetic Theory of Gases)*

With Anode Active Layer

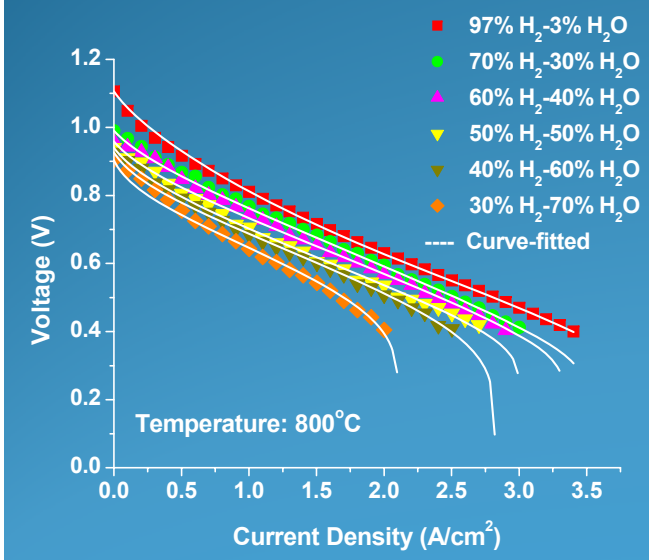

Without Anode Active Layer

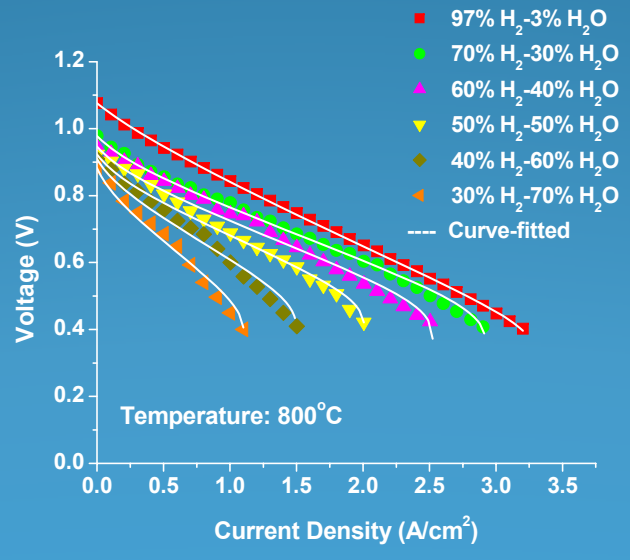

Fuel Compositions	Exchange Current Density (A/cm²)	
	With AAL	Without AAL
H_2 – 3% H_2O	0.87	0.98
H_2 – 30% H_2O	0.84	0.78
H_2 – 40% H_2O	0.82	0.70
H_2 – 50% H_2O	0.79	0.57
H_2 – 60% H_2O	0.75	0.43
H_2 – 70% H_2O	0.53	0.22

* R. Byron Bird, Warren E. Stewart, Edwin N. Lightfoot, Transport Phenomena, John Wiley & Sons (1960)

Fuel Utilization Test : Performance Analysis

- **Activation Polarization:**
  - At **Low Fuel Utilization** (H_2-3% H_2O)

    ⇒ Dominated by **Cathode**

    (No Difference in **Cell Performance** and **Exchange Current Density** due to Anode Active Layer at Low Fuel Utilization)

$$\eta_{act} \approx \eta_{act,c} = \frac{2RT}{F} \ln\left\{\frac{1}{2}\left[\left(\frac{i}{i_{0,c}}\right) + \sqrt{\left(\frac{i}{i_{0,c}}\right)^2 + 4}\right]\right\}$$

$$i_{0,a} >> i_{0,c} \qquad i_0 \approx i_{0,c}$$

  - At **High Fuel Utilization**

    ⇒ Anodic Activation Polarization Increases

    ⇒ Cathodic Activation Polarization: Independent of Fuel Composition

$$\eta_{act,a} \approx \eta_{act} - \eta_{act,c} = \frac{2RT}{F} \ln\left\{\frac{1}{2}\left[\left(\frac{i}{i_{0,a}}\right) + \sqrt{\left(\frac{i}{i_{0,a}}\right)^2 + 4}\right]\right\}$$

Fuel Utilization Test : Performance Analysis

❖ **Anodic Activation Polarization:**

$$\eta_{act,a} = \frac{2RT}{F} \ln\left\{\frac{1}{2}\left[\left(\frac{i}{i_{0,a}}\right) + \sqrt{\left(\frac{i}{i_{0,a}}\right)^2 + 4}\right]\right\}$$

With Anode Active Layer

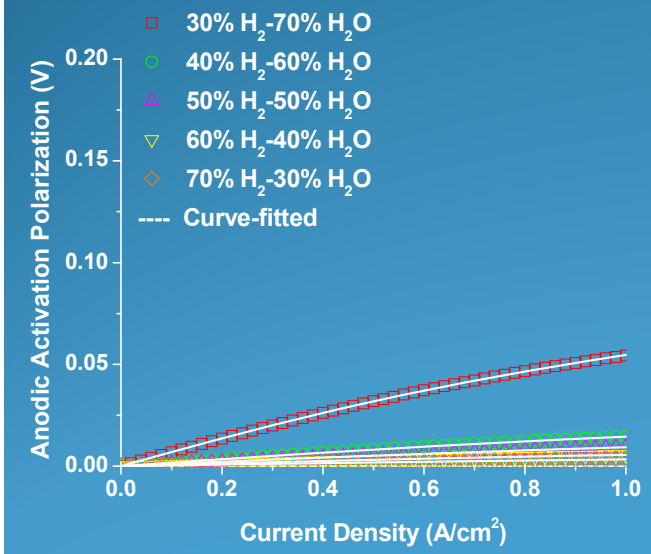

Without Anode Active Layer

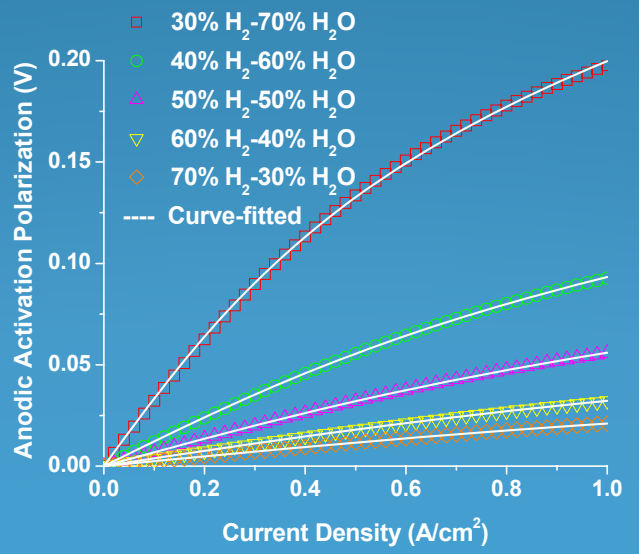

Fuel Compositions	Anodic Exchange Current Density (A/cm²)	
	With AAL	Without AAL
H_2 – 30% H_2O	26.73	4.18
H_2 – 40% H_2O	15.68	2.70
H_2 – 50% H_2O	9.47	1.53
H_2 – 60% H_2O	6.02	0.88
H_2 – 70% H_2O	1.55	0.34
Cathodic Exchange Current Density (A/cm²)	0.87	0.98

Fuel Utilization Test : Performance Analysis

❖ **Anodic Concentration Polarization:**

$$\eta_{conc,a} = \frac{RT}{4F} \ln\left(\frac{p_{O2}^{i,a}}{p_{O2}^{o,a}}\right)$$

$p^{i,a}_{O2}$: Oxygen partial pressure at anode-electrolyte interface

$p^{o,a}_{O2}$: Oxygen partial pressure outside anode surface

Determined by Local H_2-H_2O Equilibrium: $p_{O2} = \frac{p_{H2O}^2}{K p_{H2}^2}$

Calculation of $p^{i,a}_{O2}$

In Steady State, $|J_{H2}| = |J_{H2O}| = \frac{i}{2F}$ $\quad J_{H2} + J_{H2O} = 0$

$$J_{H2} = -D_{H2-H2O}^{eff} \nabla n_{H2} = -D_{H2-H2O}^{eff} \frac{p_{H2}^{i} - p_{H2}^{o}}{RTl_a} \Rightarrow p_{H2}^{i} = p_{H2}^{o} - \frac{RTl_a}{2FD_{H2-H2O}^{eff}} i$$

$$J_{H2O} = -D_{H2-H2O}^{eff} \nabla n_{H2O} = -D_{H2-H2O}^{eff} \frac{p_{H2O}^{o} - p_{H2O}^{i}}{RTl_a} \Rightarrow p_{H2O}^{i} = p_{H2O}^{o} + \frac{RTl_a}{2FD_{H2-H2O}^{eff}} i$$

Fuel Utilization Test : Performance Analysis

❖ **Anodic Concentration Polarization:**

$$\eta_{conc,a} = \frac{RT}{4F} ln\left(\frac{p_{O2}^{i,a}}{p_{O2}^{o,a}}\right)$$

$$= \frac{RT}{2F} ln\left[\frac{\left(p_{H2O}^{o,a} + \frac{RTl_a}{2FD_{H2-H2O}^{eff}} i\right) p_{H2}^{o,a}}{\left(p_{H2}^{o,a} - \frac{RTl_a}{2FD_{H2-H2O}^{eff}} i\right) p_{H2O}^{o,a}}\right]$$

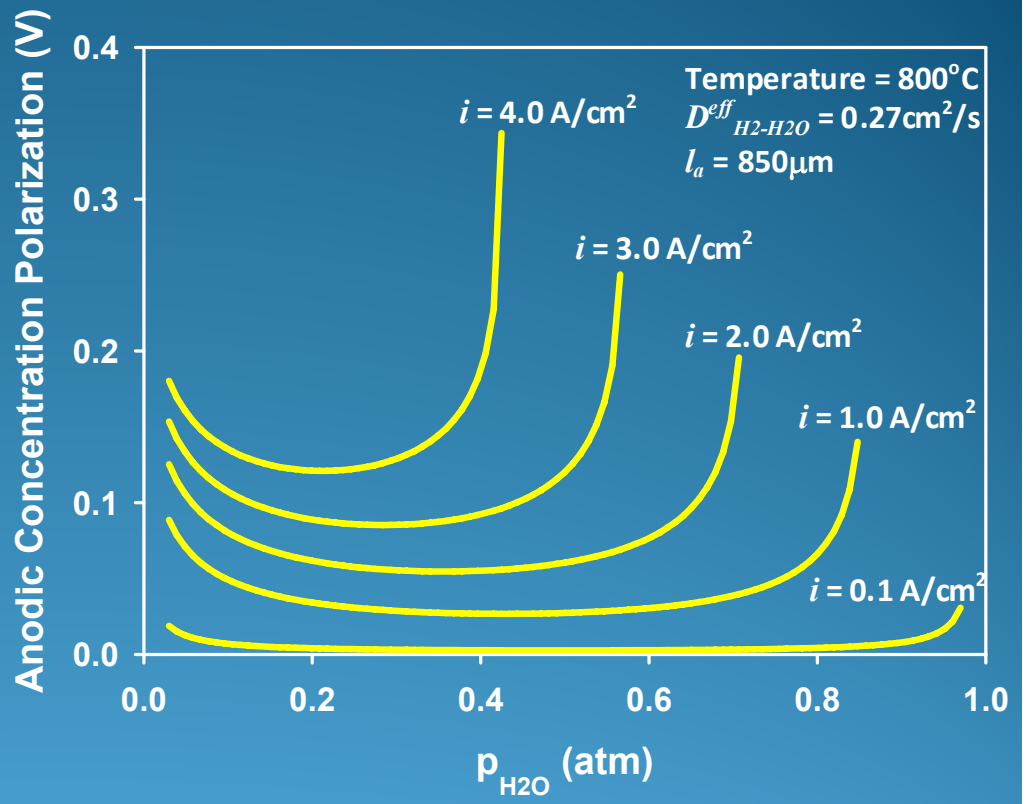

- Anodic concentration polarization is low when the fuel is in the intermediate H_2O partial pressure region.
- Anode active layer had no significant effect on anodic concentration polarization.

Fuel Utilization Test : Polarization Analysis

❖ Anodic Electrode Polarization Loss:

With Anode Active Layer

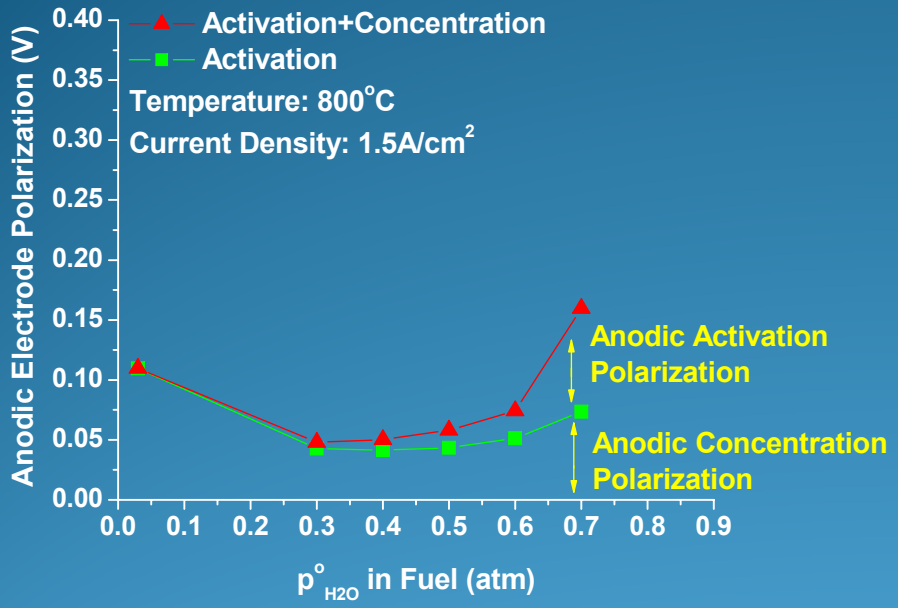

Without Anode Active Layer

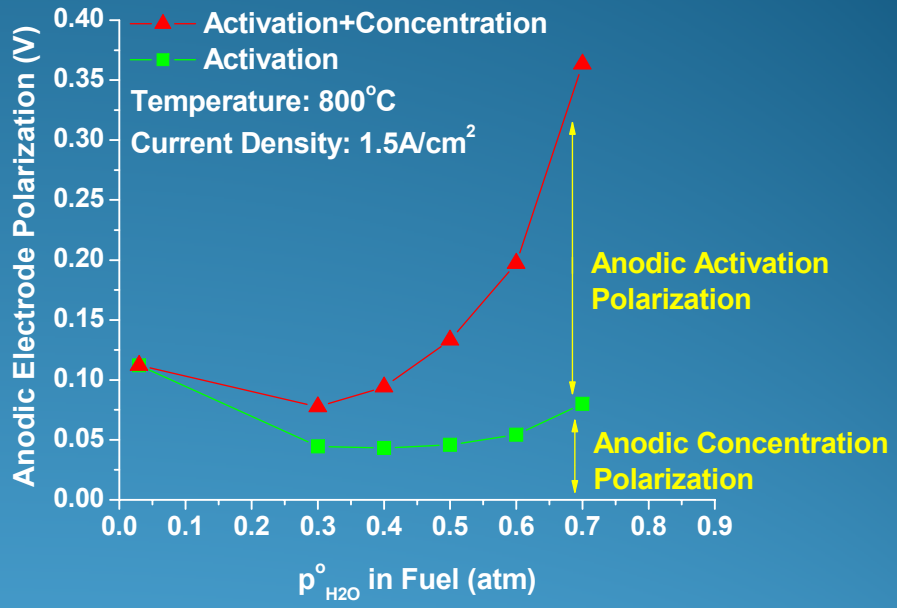

- **Activation Polarization: Dominant Loss at High Fuel Utilization**

  ⇒ **Significantly Reduced by Anode Active Layer**

Advanced Cathode Investigation : Background

- Cathode Polarization Loss : Major Difficulty in Lowering the Operating Temperature
- A site-doped Lanthanum Cobaltite
  - High Catalytic Activity and Mixed Electronic-Ionic Conductivity
  - High Thermal Expansion Coefficient
  - Solid State Reaction with YSZ at Low Temperature
- A site-doped Lanthanum Ferrite
  - High Catalytic Activity and Mixed Electronic-Ionic Conductivity
  - Adjustable Thermal Expansion
  - No Solid State Reaction with YSZ up to 1400°C
  - Diffusion of Zr^{4+} into Lanthanum Ferrite : Doped Ceria Interlayer
- Calcium-doped Lanthanum Ferrite
  - Defect Model
  - Thermogravimetry Measurements

  } p_{O2} - Weight Relationship ⇒ Equilibrium Defect Concentration
  - Electrical Conductivity Measurements ⇒ Hole Mobility

ADVANCED CATHODE INVESTIGATION : POINT DEFECT MODEL

❖ **Point Defect Model for $(La_{0.8}Ca_{0.2})_{0.95}FeO_{3-\delta}$**

A-site	B-site	O-site
La_{La}^{x}	Fe_{Fe}^{x}	O_{O}^{x}
$Ca_{La}^{'}$ = 0.2×0.95	$Fe_{Fe}^{\bullet}$	$V_{O}^{\bullet\bullet}$
$V_{La}^{'''}$ = 0.05	~~$Fe_{Fe}^{'}$~~ ≈ 0	
	~~$V_{Fe}^{'''}$~~ ≈ 0	

- **Oxygen Incorporation Reaction**

$$V_O^{\bullet\bullet} + 2Fe_{Fe}^{x} + \frac{1}{2}O_2 \leftrightarrow O_O^{x} + 2Fe_{Fe}^{\bullet} \quad \Longrightarrow \quad K_{ox} = \frac{[O_O^{x}][Fe_{Fe}^{\bullet}]^2}{[V_O^{\bullet\bullet}][Fe_{Fe}^{x}]^2 p_{O2}^{1/2}}$$

- **Charge Disproportionation Reaction**

$$2Fe_{Fe}^{x} \leftrightarrow Fe_{Fe}^{\bullet} + Fe_{Fe}^{'} \quad \Longrightarrow \quad [Fe_{Fe}^{'}] \approx 0 \ @ \ 0.001\text{atm} \leq p_{O2} \leq 1\text{atm}$$

- **Schottky Equilibrium Reaction**

$$ntl \leftrightarrow V_{La}^{'''} + V_{Fe}^{'''} + 3V_O^{\bullet\bullet} \quad \Longrightarrow \quad [V_{Fe}^{'''}] \approx 0$$

Advanced Cathode Investigation : Point Defect Model

- **Charge Neutrality Condition**

$$2[V_O^{\bullet\bullet}] + [Fe_{Fe}^{\bullet}] = [Ca_{La}'] + 3[V_{La}'''] \Longrightarrow [Fe_{Fe}^{\bullet}] = [Ca_{La}'] + 3[V_{La}'''] - 2[V_O^{\bullet\bullet}]$$

$= 0.2 \quad 0.95 \qquad = 0.05$

- **A-site Restriction**

$$[La_{La}^{x}] + [Ca_{La}'] + [V_{La}'''] = 1$$

- **B-site Restriction**

$$[Fe_{Fe}^{x}] + [Fe_{Fe}^{\bullet}] = 1 \Longrightarrow [Fe_{Fe}^{x}] = 1 - [Fe_{Fe}^{\bullet}] = 1 - [Ca_{La}'] - 3[V_{La}'''] + 2[V_O^{\bullet\bullet}]$$

$= 0.2 \times 0.95 \qquad = 0.05$

- **O-site Restriction**

$$[O_O^{x}] + [V_O^{\bullet\bullet}] = 3 \Longrightarrow [O_O^{x}] = 3 - [V_O^{\bullet\bullet}]$$

- **Mass Action Coefficient for Oxygen Exchange Reaction**

$$K_{ox} = \frac{[O_O^{x}][Fe_{Fe}^{\bullet}]^2}{[V_O^{\bullet\bullet}][Fe_{Fe}^{x}]^2 p_{O2}^{1/2}}$$

$$K_{ox} = \frac{(3 - [V_O^{\bullet\bullet}])([Ca_{La}'] + 3[V_{La}'''] - 2[V_O^{\bullet\bullet}])^2}{[V_O^{\bullet\bullet}](1 - [Ca_{La}'] - 3[V_{La}'''] + 2[V_O^{\bullet\bullet}])^2} \cdot \frac{1}{p_{O2}^{1/2}}$$

ADVANCED CATHODE INVESTIGATION : POINT DEFECT MODEL

- Relationship between p_{O2} and Weight of $(La_{0.8}Ca_{0.2})_{0.95}FeO_{3-\delta}$

$$K_{ox} = \frac{(3-[V_O^{\bullet\bullet}])([Ca_{La}{}'] + 3[V_{La}{}'''] - 2[V_O^{\bullet\bullet}])^2}{[V_O^{\bullet\bullet}](1-[Ca_{La}{}'] - 3[V_{La}{}'''] + 2[V_O^{\bullet\bullet}])^2} \cdot \frac{1}{p_{O2}^{1/2}}$$

$$M_{LCF} = n \times m_{LCF} = n \times [(0.8 \times m_{La} + 0.2 \times m_{Ca}) \times 0.95 + m_{Fe} + (3-\delta) \times m_O]$$

$$\delta = [V_O^{\bullet\bullet}] = 13.56 - 0.0625 \times \frac{M_{LCF}}{n}$$

$$p_{O2} = \frac{1}{K_{ox}^2} \times \frac{\left(-10.56 + 0.0625 \times \frac{M_{LCF}}{n}\right)^2 \left(-26.78 + 0.125 \times \frac{M_{LCF}}{n}\right)^4}{\left(13.56 - 0.0625 \times \frac{M_{LCF}}{n}\right)^2 \left(27.78 + 0.125 \times \frac{M_{LCF}}{n}\right)^4}$$

ADVANCED CATHODE INVESTIGATION : THERMOGRAVIMETRY

Thermogravimetry Measurements

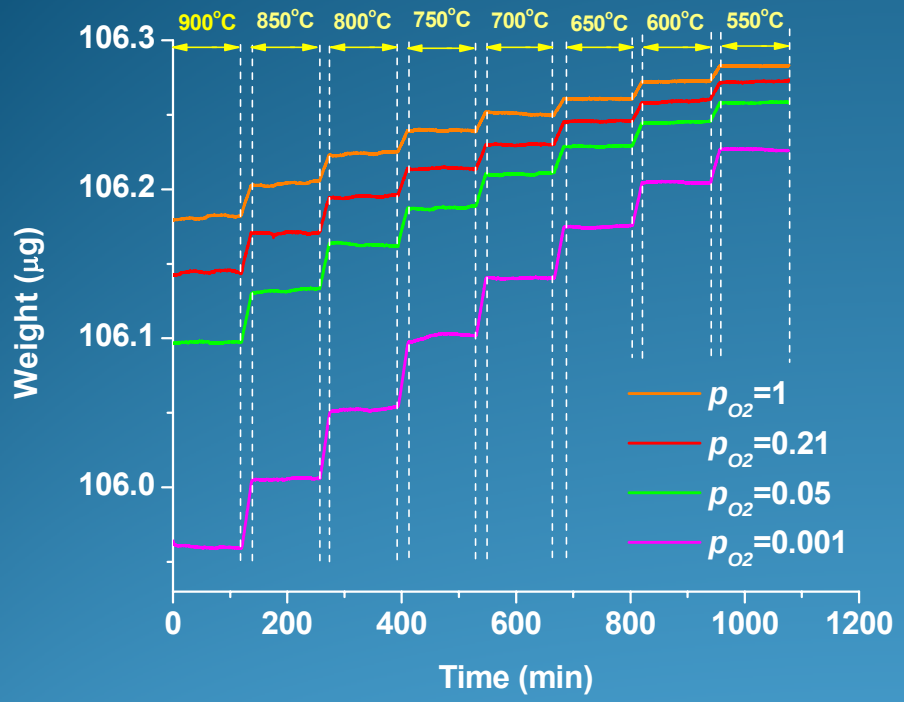

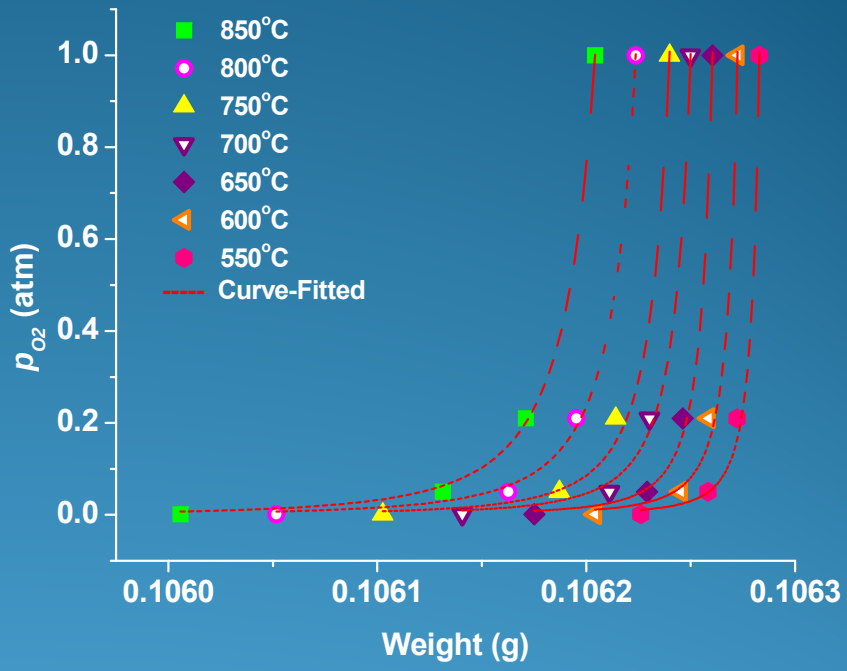

$$p_{O2} = \frac{1}{K_{ox}^2} \times \frac{\left(-10.56 + 0.0625 \times \frac{M_{LCF}}{n}\right)^2 \left(-26.78 + 0.125 \times \frac{M_{LCF}}{n}\right)^4}{\left(13.56 - 0.0625 \times \frac{M_{LCF}}{n}\right)^2 \left(27.78 + 0.125 \times \frac{M_{LCF}}{n}\right)^4}$$

→ ***n* = 0.00049 mol**

Temperature	850°C	800°C	750°C	700°C	650°C	600°C	550°C
K_{ox}	186	235	317	376	504	630	813

ADVANCED CATHODE INVESTIGATION : DEFECT EQUILIBRIUM

- Equilibrium Defect Concentration

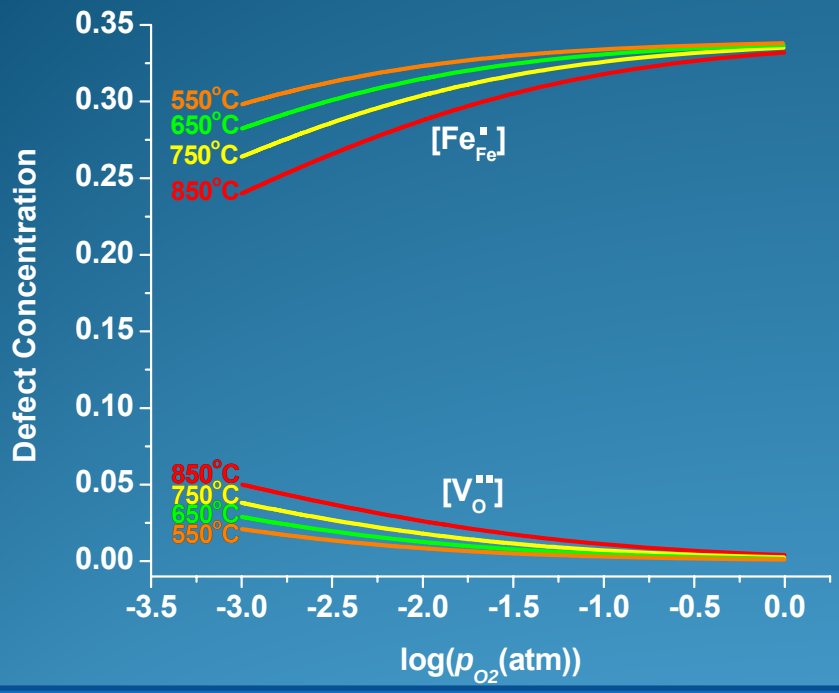

- $ln(K_{ox})$ vs. 1/T

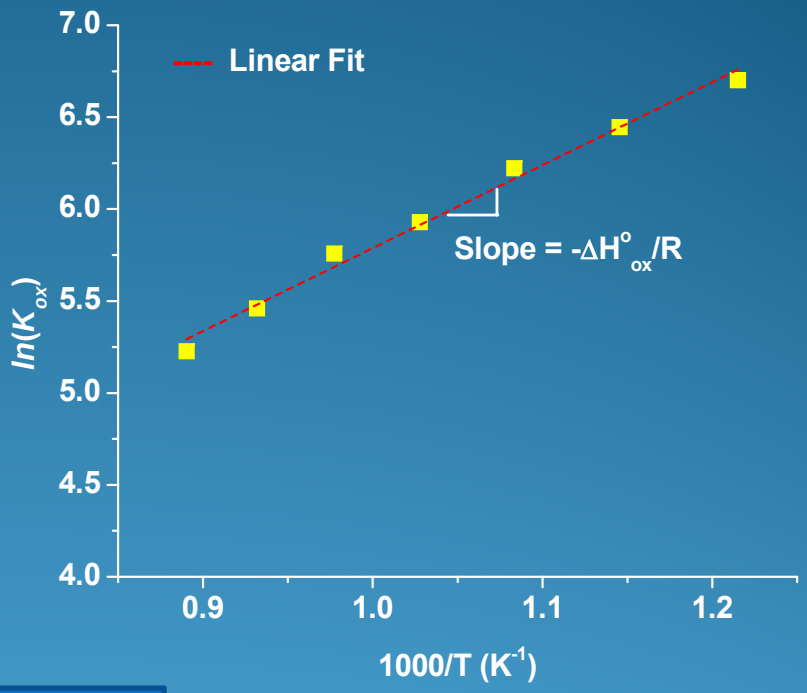

- **High p_{O2} range**
  - $[V_O^{\bullet\bullet}]$: low
  - Charge neutrality is maintained by hole formation.
- **Low p_{O2} range**
  - $[V_O^{\bullet\bullet}]$: high
  - Hole concentration decreases.

$$ln(K_{ox}) = -\frac{\Delta H^o_{ox}}{RT} + \frac{\Delta S^o_{ox}}{R}$$

ΔH^o_{ox} = -37.5 kJ mol^{-1}

ΔS^o_{ox} = 10.6 J mol^{-1} K^{-1}

Advanced Cathode Investigation : Electrical Conductivity

Electrical Conductivity Measurements

Conductivity vs. Temperature

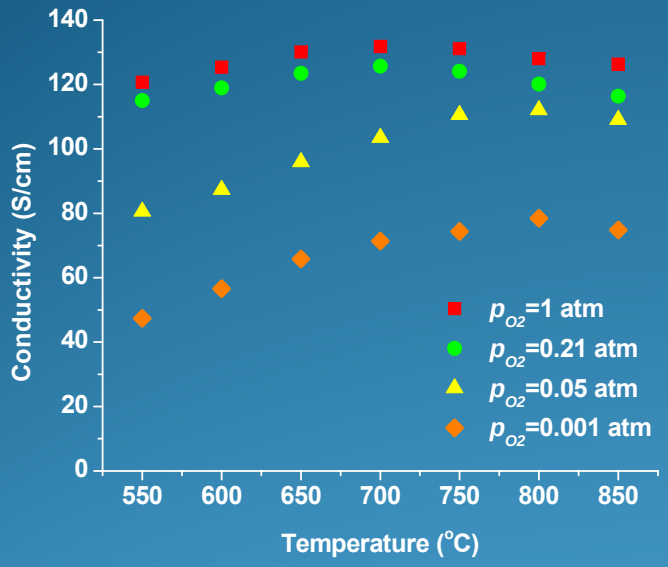

$$\sigma_t = \sigma_e + \sigma_i \approx \sigma_e$$

- $p_{O2}\uparrow \Rightarrow \sigma_e \uparrow$: *p*-type conductor
- Low Temperature: Thermally Activated Behavior (Small Polaron Hopping)
- High Temperature: Decrease in Hole Concentration

Mobility vs. Temperature

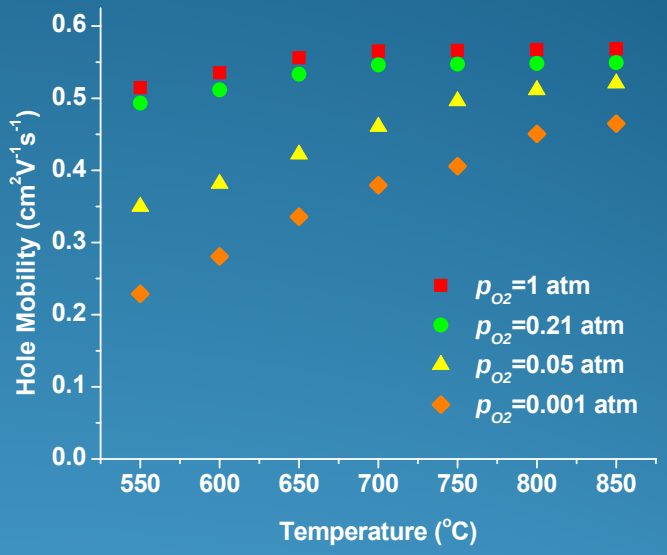

$$\sigma_p = \frac{[Fe_{Fe}^{\bullet}]}{V} q\,\mu_p$$

- $p_{O2}\downarrow$, T $\uparrow \Rightarrow [V_O^{\cdot\cdot}] \uparrow$
- Hopping Conduction Via Fe^{4+}-O-Fe^{3+} Chain
- $V_O^{\cdot\cdot}$: Scattering Centers or Random Traps for Electrons

Advanced Cathode Investigation : Conduction Mechanism

- **Adiabatic Small Polaron Hopping**

$$\mu_p = \frac{(1 - [Fe_{Fe}^{\bullet}])qa^2\nu}{kT} \exp\left(-\frac{E_A}{kT}\right)$$

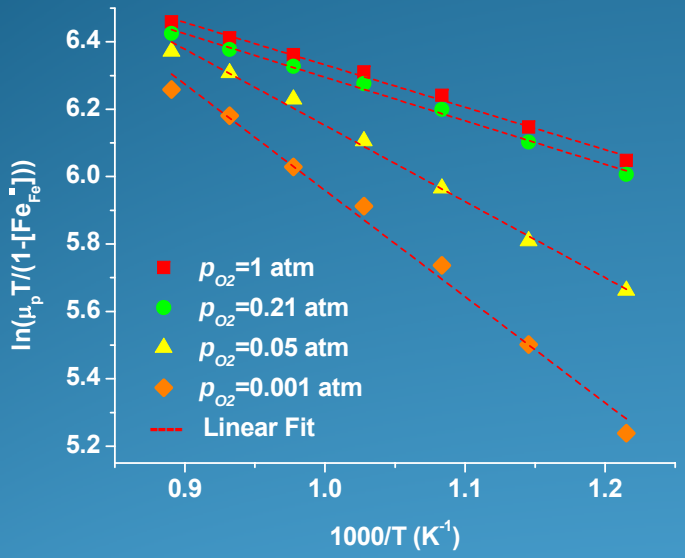

- **Non-adiabatic Small Polaron Hopping**

$$\mu_p = \frac{(1 - [Fe_{Fe}^{\bullet}])qa^2}{kT} P \exp\left(-\frac{E_A}{kT}\right)$$

$$P = \frac{J^2}{2\hbar}\left(\frac{\pi}{E_A kT}\right)^{1/2}$$

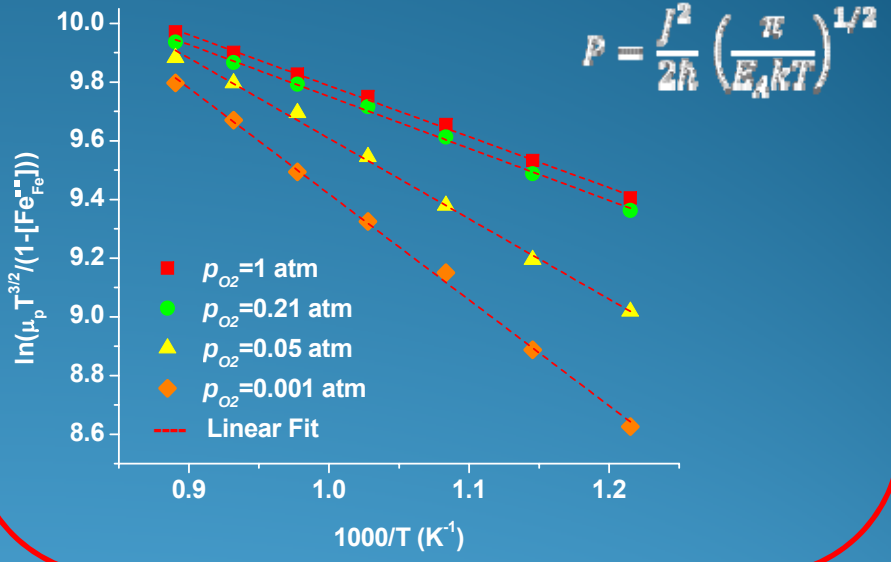

p_{O2} (atm)	Adiabatic Case		Non-adiabatic Case	
	Activation Energy (eV)	R^2	Activation Energy (eV)	R^2
1	0.108	0.99353	0.149	0.99788
0.21	0.111	0.99344	0.152	0.99776
0.05	0.195	0.99423	0.235	0.99673
0.001	0.272	0.98927	0.310	0.99801

BOSTON UNIVERSITY

SUMMARY

- Successfully developed single-step un-constrained co-firing of the solid oxide fuel cell @ 1300°C.
- Modeled cell performance.
- Achieved maximum power density of 1.50 W/cm^2 at 800°C and 0.87 W/cm^2 at 700°C with humidified hydrogen (3% H_2O) and air.
- Simulated the effect of practical fuel utilization on single cell performance.
- Improved cell performance at high fuel utilization by employing anode active layer.
- Investigated defect chemistry and electrical conduction mechanism of novel cathode material (calcium-doped lanthanum ferrite).

FUTURE WORK

- Employ advanced cathode material in co-firing process.
- Analyze performance at low operating temperature (600-700°C).

PUBLICATION LIST

BOSTON UNIVERSITY

Journal Papers

1. Kyung Joong Yoon, Wenhua Huang, Guosheng Ye, Srikanth Gopalan, Uday B. Pal, Donald A. Seccombe, Jr., "Electrochemical Performance of Solid Oxide Fuel Cells (SOFCs) Manufactured by Single Step Co-firing Process," *Journal of the Electrochemical Society*, 154 (4) B389 (2007).
2. Kyung Joong Yoon, Srikanth Gopalan, Uday B. Pal, "Effect of Fuel Composition on Performance of Single Step Co-fired Solid Oxide Fuel Cells (SOFCs)," *Journal of the Electrochemical Society*, 154 (10) B1080 (2007).
3. Kyung Joong Yoon, Peter Zink, Srikanth Gopalan, Uday B. Pal, "Polarization Measurements on Single Step Co-fired Solid Oxide Fuel Cells (SOFCs)," *Journal of Power Sources*, 172 (1) 39 (2007).
4. Kyung Joong Yoon, Srikanth Gopalan, Uday B. Pal, "Effect of Anode Active Layer on Performance of Single Step Co-fired Solid Oxide Fuel Cells (SOFCs) at High Fuel Utilizations," *Journal of the Electrochemical Society*, 155(6) B610 (2008).
5. Kyung Joong Yoon, Srikanth Gopalan, Uday B. Pal, "Analysis of Electrochemical Performance of Solid Oxide Fuel Cells (SOFCs) Using Polarization Modeling and Impedance Measurements," *Journal of the Electrochemical Society*, 156 (3) B311 (2008).
6. Kyung Joong Yoon, Guosheng Ye, Srikanth Gopalan, Uday B. Pal, "Cost-effective Single Step Co-firing Technique for Manufacturing Solid Oxide Fuel Cells (SOFCs) using High Shear Compaction (HSC) Anode," *Journal of Fuel Cell Science and Technology*, Accepted (2008).
7. Soobhankar Pati, Kyung Joong Yoon, Uday B. Pal, "Solid Oxide Electrolyte Electrolyzer with Liquid Metal Anode for Production of Hydrogen and Syn-Gas from Waste and Steam," submitted (2009).
8. Kyung Joong Yoon, Peter Zink, Larry Pederson, Srikanth Gopalan, Uday B. Pal, "Defect Chemistry and Electrical Properties of $(La_{0.8}Ca_{0.2})_{0.95}FeO_{3-\delta}$," in preparation (2009).

Conference Proceedings

1. Kyung Joong Yoon, Peter Zink, Srikanth Gopalan, Uday B. Pal, "Polarization Analysis in Single Step Co-fired Solid Oxide Fuel Cells (SOFCs)," *Materials Research Society Symposium Proceedings of the Fall 2006 Meeting*, Vol. 972, AA 10-02 (2007).
2. Peter A. Zink, Kyung Joong Yoon, Wenhua Huang, Srikanth Gopalan, Uday B. Pal, Donald A. Seccombe, Jr., "Refractory Cathode Investigation for Single Step Co-fired Solid Oxide Fuel Cells (SOFCs)," *Materials Research Society Symposium Proceedings of the Fall 2006 Meeting*, Vol. 972, AA 03-12 (2007).
3. Kyung Joong Yoon, Peter Zink, Uday B. Pal, Srikanth Gopalan, "High Performance Low Cost Co-fired Solid Oxide Fuel Cells (SOFCs)," *ECS Transactions*, Vol. 7 (1) 579 (2007).
4. Kyung Joong Yoon, Srikanth Gopalan, Uday B. Pal, "Anode Polarization Effects in Single Step Co-fired Solid Oxide Fuel Cells (SOFCs)," *ECS Transactions*, Vol. 7 (1) 565 (2007).
5. Peter Zink, Kyung Joong Yoon, Wenhua Huang, Uday B. Pal, Srikanth Gopalan, "Refractory Cathode Investigation for Single Step Co-fired Solid Oxide Fuel Cells (SOFCs)," *ECS Transactions*, Vol. 7 (1) 399 (2007).
6. Kyung Joong Yoon, Srikanth Gopalan, Uday B. Pal, "Effect of Anode Active Layer on Performance of Single Step Co-fired Solid Oxide Fuel Cells (SOFCs)," *ECS Transactions*, Vol. 13 (26) 249 (2008).
7. Kyung Joong Yoon, Srikanth Gopalan, Uday B. Pal, "Electrochemical Performance of Single Step Co-Fired Solid Oxide Fuel Cells (SOFCs) Analyzed Using Polarization Modeling and Impedance Spectroscopy," *Materials Research Society Symposium Proceedings of the Fall 2008 Meeting*, Vol. 1126, S10-02 (2008).
8. Peter A. Zink, Kyung Joong Yoon, Uday B. Pal, Srikanth Gopalan, "Electrical Performance of Calcium-doped Lanthanum Ferrite for Use in Single Step Co-Fired Solid Oxide Fuel Cells (SOFCs)," *Materials Research Society Symposium Proceedings of the Fall 2008 Meeting*, Vol. 1126, S11-02 (2008).

BOSTON UNIVERSITY

Thank you!